

[W₆S₈] Octahedral Tungsten Clusters Functionalized with Thiophene Derivatives: toward Polymerizable Building Blocks

Sandrine Perruchas,^{*,†,‡} Samuel Flores,[†] Bruno Jousset,[§] Emil Lobkovsky,[†] Hector Abruña,[†] and Francis J. DiSalvo^{*,†}

Department of Chemistry and Chemical Biology, Baker Laboratory, Cornell University, Ithaca, New York 14853-1301, and Chimie des Surfaces et Interfaces, CEA Saclay, 91191 Gif-sur-Yvette, France

Received June 1, 2007

The functionalization of octahedral [W₆S₈] clusters with a family of phosphino–thiophene ligands has been investigated with the goal of synthesizing extended networks of [W₆S₈] units covalently linked to one another through thiophene-conjugated bridges. In addition to new phosphino–thiophene ligands, eight clusters were synthesized and characterized by ¹H and ³¹P NMR spectroscopies, elemental analysis, and UV–vis absorption. These clusters are formulated [W₆S₈(T–PPh₂)₆] (**1a**), [W₆S₈(T–PEt₂)₆] (**1b**), [W₆S₈(2T–PPh₂)₆] (**2a**), [W₆S₈(2T–PEt₂)₆] (**2b**), [W₆S₈(3T–PPh₂)₆] (**3a**), [W₆S₈(3T–PEt₂)₆] (**3b**), [W₆S₈((2T)₃P)₆] (**4**), and [W₆S₈(2EDOT–PEt₂)₆] (**5**) (T = thiophene and EDOT = 3,4-ethylenedioxythiophene). The molecular structure of six of them has been obtained by single-crystal X-ray diffraction analysis. All of them crystallize in the *P* $\bar{1}$ triclinic space group except **3b**, which has the *P*2₁/*c* monoclinic symmetry. The redox behavior of both the ligands and the corresponding functionalized clusters has been investigated by cyclic voltammetry. An attempt to electropolymerize these species is also reported.

Introduction

Since their discovery more than 30 years ago, the Chevrel phases M'_x[Mo₆Q₈] (M' = Pb, Sn, Cu, ...; X = S, Se, Te) have been intensively studied due to various properties including superconductivity, high thermoelectric figures of merit, fast-ionic conductivity, and catalytic activity.¹ The Chevrel phases are built of octahedral molybdenum chalcogenide units formulated [Mo₆Q₈] and connected to one another by M–Q bonds. Surprisingly, no tungsten analogues of the Chevrel phases have ever been reported. However, molecular tungsten clusters formulated [W₆S₈L₆]² have been obtained in solution in analogy with the molybdenum species [Mo₆S₈L₆].³ These clusters can be described as octahedra of metallic atoms (M = Mo, W) with their faces capped by

eight triply bridging sulfur atoms and six terminal ligands (L) to complete the coordination sphere of the M atoms (Scheme 1). The terminal ligands of these soluble molecular forms can be exchanged by a variety of other ligands.

Theoretical work has shown that extended networks based on [W₆Q₈] units covalently linked together by π -conjugated ditopic ligands might exhibit interesting electronic properties due to electronic communication through the networks.^{4,5} We are interested in preparing such organic–inorganic hybrid materials, and several directions have been pursued. One way is to replace the monodentate ligands (L) on the clusters with ditopic ligands such as 4-4'-bipyridine. Unfortunately, these coordination experiments systematically led to insoluble amorphous products. The characterization of these products was thus very difficult, and it is even possible that the product precipitated before complete hexasubstitution of the [W₆Q₈] unit occurred. Other attempts using clusters with mixed axial ligands that have different binding energies gave the same

* To whom correspondence should be addressed. E-mail: sandrine.perruchas@polytechnique.edu (S.P.), fjd3@cornell.edu (F.J.D.).

[†] Cornell University.

[‡] Present address: Laboratoire de Physique de la Matière Condensée, CNRS, Ecole Polytechnique, 91128 Palaiseau, France.

[§] CEA Saclay.

(1) (a) Chevrel, R.; Sergent, M.; Prigent, J. *J. Solid State Chem.* **1971**, *3*, 515–519. (b) Chevrel, R.; Hirrien, M.; Sergent, M. *Polyhedron* **1986**, *5*, 87–94.

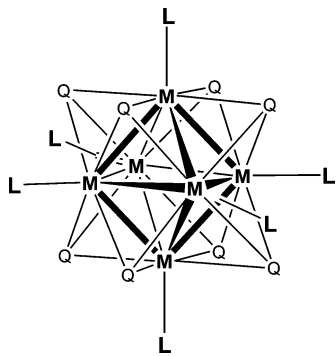
(2) Saito, T.; Yoshikawa, A.; Yamagata, T.; Imoto, H.; Unoura, K. *Inorg. Chem.* **1989**, *28*, 3588–3592.

(3) (a) Saito, T.; Yamamoto, N.; Yamagata, T.; Imoto, H. *J. Am. Chem. Soc.* **1988**, *110*, 1646–1647. (b) Saito, T.; Yamamoto, N.; Nagase, T.; Tsuboi, T.; Kobayashi, K.; Yamagata, T.; Imoto, H.; Unoura, K. *Inorg. Chem.* **1990**, *29*, 764–770.

(4) Hughbanks, T.; Hoffman, R. *J. Am. Chem. Soc.* **1983**, *105*, 1150–1162.

(5) Malik, A.-S. Thesis, Cornell University, Ithaca, NY, 1998.

Scheme 1. General Representation of $[M_6Q_8L_6]$ Clusters (M = W, Mo; Q = S; and L = Phosphinothiophene Derivatives for the Clusters Studied)



result. However, it is worth noting that different types of extended networks of $[W_6Q_8]$ units have been obtained in crystalline form. One example is a coordination network composed of $[W_6Q_8(CN)_6]^{6-}$ and transition metals.⁶ The other example is a supramolecular three-dimensional (3D) network of $[W_6Q_8L_6]$ clusters (L = pyridine-based ligands) linked through hydrogen bonds.⁷

Here, we investigate a different approach based on organic polymerization to synthesize such hybrid cluster–organic covalently bonded networks. Polythiophene is a well-known organic π -conjugated polymer with interesting properties including high conductivity. Considerable research efforts have been invested, largely motivated by the multiple potential technological applications such as electrochemical sensors, photovoltaic devices, organic field-effect transistors, electrical-energy storage devices, or electrooptical systems.⁸ The synthesis of the polythiophene polymer is easily achieved by chemical or electrochemical oxidation of the corresponding oligomer. Many thiophene oligomers have been synthesized with different functional groups. Among them, the use of coordinative groups such as carboxylic acids,^{9–11} terpyridine,¹² bipyridine,¹³ or pyridine,¹⁴ for example, has been developed to attach metallic complexes to the thiophene backbone in order, in some cases, to modify and possibly tune the electronic and optical properties of the resulting polymer. For this purpose, complexes incorporating phosphino–terthiophene ligands^{15,16} have been mainly de-

veloped by the groups of Mirkin^{17,18} and Wolf.^{19–23} The electropolymerization of such palladium, iron, and ruthenium complexes led to materials in which metal groups are coupled to the thiophene backbone.

By taking advantage of both the well-documented phosphine functionalization of $[M_6Q_8]$ (M = Re, Mo, W; Q = S, Se) cluster cores^{2,3,24–28} and our experience in this field,^{29–35} phosphino–thiophene derivatives appeared to be good ligands for our study. The phosphine functionalized clusters are quite inert toward ligand exchange reactions, which makes them relatively stable in solution. Once the cluster is functionalized by the thiophene ligands, it can then be polymerized to obtain materials where the $[W_6Q_8]$ units are covalently linked to one another leading to a 3D network. In such polymers, the metal centers may be involved in the charge transport through the conjugated organic chains (Scheme 2). Due to the octahedral symmetry of the cluster core, a polymer of high dimensionality can be expected, and this kind of compound could have interesting electronic properties.

It is worth noting that organic polymers incorporating molybdenum and rhenium octahedral clusters have been already reported. One example is the incorporation of $[M_6Cl_8]^{4+}$ moieties into poly(4-vinylpyridine) polymer.^{36,37} The one-dimensional $LiMo_3Se_3$ compound based on condensed Mo_6 units has been also immobilized in a vinylene carbonate

(6) Jin, S.; DiSalvo, F. J. *Chem. Mater.* **2002**, *14*, 3448–3457.

(7) Oertel, C. M.; Sweeder, R. D.; Patel, S.; Downie, C. M.; DiSalvo, F. J. *Inorg. Chem.* **2005**, *44*, 2287–2296.

(8) Roncali, J. *Chem. Rev.* **1992**, *92*, 711–738.

(9) Kuroda-Sowa, T.; Nogami, T.; Konaka, H.; Maekawa, M.; Munataka, M.; Miyasaka, H.; Yamashita, M. *Polyhedron* **2003**, *22*, 1795–1801.

(10) Lim, J. M.; Do, Y.; Kim, J. *Eur. J. Inorg. Chem.* **2006**, 711–717.

(11) Ni, Z.; Yassar, A.; Antoun, T.; Yaghi, O. M. *J. Am. Chem. Soc.* **2005**, *127*, 12752–12753.

(12) Encinas, S.; Flamigni, L.; Barigelletti, F.; Constable, E. C.; Housecroft, C. E.; Schofield, E. R.; Figgemeier, E.; Fenske, D.; Neuburger, M.; Vos, J. G.; Zehnder, M. *Chem.–Eur. J.* **2002**, *8*, 137–150.

(13) Jousset, B.; Blanchard, P.; Ocafrain, M.; Allain, M.; Levillain, E.; Roncali, J. *J. Mater. Chem.* **2004**, *14*, 421–427.

(14) Constable, E. C.; Housecroft, C. E.; Neuburger, M.; Schmitt, C. X. *Polyhedron*, **2006**, *25*, 1844–1863.

(15) Baumgartner, T.; Réau, R. *Chem. Rev.* **2006**, *106*, 4681–4727.

(16) Field, J. S.; Haines, R. J.; Lakoba, E. I.; Sosabowski, M. H. *J. Chem. Soc., Perkin Trans. 1* **2001**, 3352–3360.

(17) Weinberger, D. A.; Higgins, T. B.; Mirkin, C. A.; Liable-Sands, L. M.; Rheingold, A. L. *Angew. Chem., Int. Ed.* **1999**, *38*, 17, 2565–2568.

(18) Weinberger, D. A.; Higgins, T. B.; Mirkin, C. A.; Stern, C. L.; Liable-Sands, L. M.; Rheingold, A. L. *J. Am. Chem. Soc.* **2001**, *123*, 2503–2516.

(19) Stott, T. L.; Wolf, M. O. *Coord. Chem. Rev.* **2003**, *246*, 89–101.

(20) Moorlag, C.; Sih, B. C.; Stott, T. L.; Wolf, M. O. *J. Mater. Chem.* **2005**, *15*, 2433–2436.

(21) Clot, O.; Wolf, M. O.; Patrick, B. O. *J. Am. Chem. Soc.* **2001**, *123*, 9963–9973.

(22) Clot, O.; Wolf, M. O.; Patrick, B. O. *J. Am. Chem. Soc.* **2000**, *122*, 10456–10457.

(23) Clot, O.; Akahori, Y.; Moorlag, C.; Leznoff, D. B.; Wolf, M. O.; Batchelor, R. J.; Patrick, B. O.; Ishii, M. *Inorg. Chem.* **2003**, *42*, 2704–2713.

(24) Saito, T.; Nishida, M.; Yamagata, T.; Yamagata, Y.; Yamaguchi, Y. *Inorg. Chem.* **1986**, *25*, 1111–1117.

(25) Zheng, Z.; Long, J. R.; Holm, R. H. *J. Am. Chem. Soc.* **1997**, *119*, 2163–2171.

(26) Willer, M. W.; Long, J. R.; McLauchlan, C. C.; Holm, R. H. *Inorg. Chem.* **1998**, *37*, 328–333.

(27) Chen, Z. N.; Yoshimura, T.; Abe, M.; Sasaki, Y.; Ishisaka, S.; Kim, S.; Kitamura, H. B. *Angew. Chem., Int. Ed.* **2001**, *40*, 1, 239–242.

(28) Tulskey, E. G.; Long, J. R. *Inorg. Chem.* **2001**, *40*, 6990–7002.

(29) Perruchas, S.; Avarvari, N.; Rondeau, D.; Levillain, E.; Batail, P. *Inorg. Chem.* **2005**, *44*, 3459–3465.

(30) Yuan, M.; Ulgüt, B.; McGuire, M.; Takada, K.; DiSalvo, F. J.; Lee, S.; Abuña, H. *Chem. Mater.* **2006**, *18*, 4296–4306.

(31) Oertel, C. M.; Rayburn, L. L.; Jin, S.; DiSalvo, F. J. *C. R. Chim.* **2005**, *8*, 1779–1788.

(32) Jin, S.; Popp, F.; Boettcher, S. W.; Yuan, M.; Oertel, C. M.; DiSalvo, F. J. *J. Chem. Soc., Dalton Trans.* **2002**, 3096–3100.

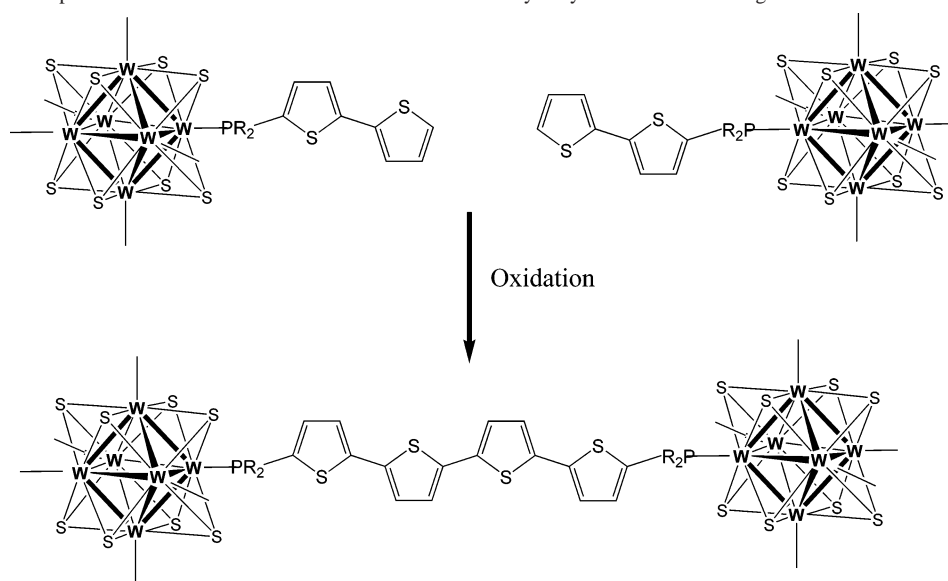
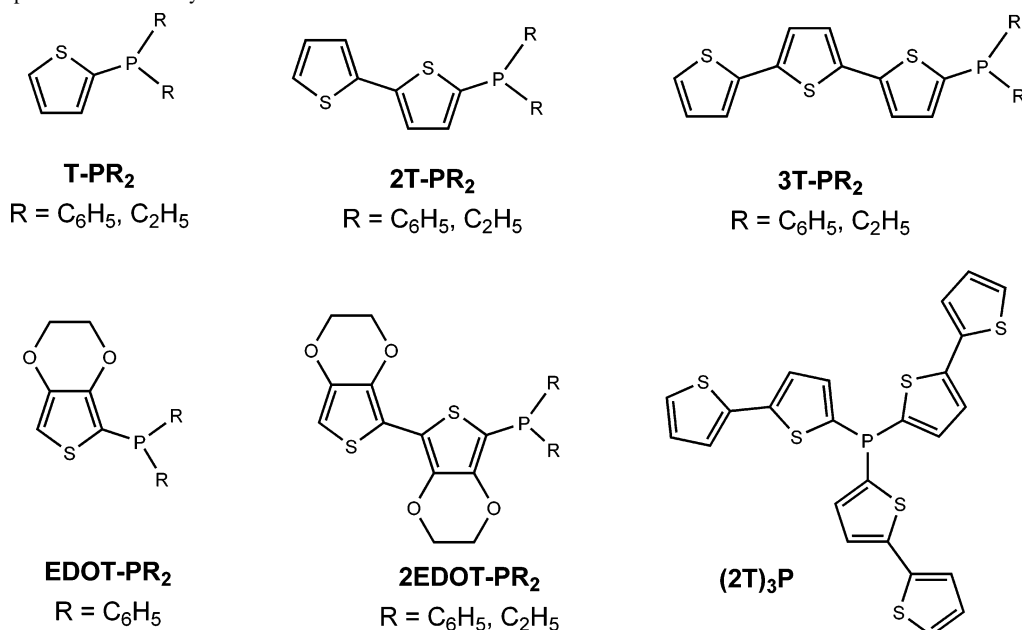
(33) Ehrlich, G. M.; Deng, H.; Hill, L. I.; Steigerwald, M. L.; Squattrito, P. J.; DiSalvo, F. J. *Inorg. Chem.* **1995**, *34*, 2480–2482.

(34) Jin, S.; Venkataraman, D.; DiSalvo, F. J. *Inorg. Chem.* **2000**, *39*, 2747–2757.

(35) Jin, S.; Zhou, R.; Scheuer, E. M.; Adamchuck, J.; Rayburn, L. L.; DiSalvo, F. J. *Inorg. Chem.* **2001**, *40*, 2666–2674.

(36) Jackson, J. A.; Newsham, M. D.; Worsham, C.; Nocera, D. G. *Chem. Mater.* **1996**, *8*, 558–564.

(37) Robinson, L. M.; Shriver, D. F. *J. Coord. Chem.* **1996**, *37*, 119–129.

Scheme 2. Schematic Representation of Possible Connection of the Clusters by Polymerization of the Ligands**Scheme 3.** Thiophene Derivatives Synthesized and Nomenclature

matrix.³⁸ More recently, a cluster bearing one 4-vinylpyridine ligand formulated $[\text{Re}_6\text{Se}_8(\text{PEt}_3)_5(4\text{-vinylpyridine})]^{2+}$ has been copolymerized with styrene.³⁹ Our approach differs from all these examples in the use of the functionalized cluster itself as a polymerizable unit and not its incorporation in a polymer matrix.

The phosphino–thiophene ligands studied are presented in Scheme 3 (T = thiophene and EDOT = 3,4-ethylenedioxythiophene). As the polymerization takes place in solution, good solubility of the clusters is required, which mainly depends on the ligands. Phosphino–thiophene derivatives are reported to be highly soluble in common organic solvents. These molecules bear the phosphine groups in

terminal position of the thiophene moiety, leaving the other carbon atom in an α position accessible to polymerization. Indeed, the α – α coupling has been reported to be the most favorable in the polymerization of thiophene derivatives.⁸ Note that the clusters $[\text{W}_6\text{S}_8(\text{T-PR}_2)_6]$ (R = Ph, Et) functionalized by ligands bearing only one thiophene unit were not expected to polymerize because of the high polymerization potential and the reduced accessibility of the α position. However, they were synthesized to be used as references for the UV–vis and electrochemical studies by comparison with the clusters functionalized by ligands bearing longer thiophene chains.

Here, we report on the synthesis of eight tungsten clusters functionalized with phosphino–thiophene derivatives. The cluster formulas are listed in Chart 1. The redox and UV–vis absorption properties of the clusters have been studied

(38) Golden, J. H.; DiSalvo, F. J.; Fréchet, J. M. J.; Silcox, J.; Thomas, M.; Elman, J. *Science* **1996**, *273*, 782–784.

(39) Roland, B. K.; Flora, W. H.; Carducci, M. D.; Armstrong, N. R.; Zheng, Z. *J. Cluster Sci.* **2003**, *14*, 4, 449–458.

Chart 1. Designation of the Clusters Synthesized

$[\text{W}_6\text{S}_8(\text{T}-\text{PPh}_2)_6]$	1a
$[\text{W}_6\text{S}_8(\text{T}-\text{PEt}_2)_6]$	1b
$[\text{W}_6\text{S}_8(2\text{T}-\text{PPh}_2)_6]$	2a
$[\text{W}_6\text{S}_8(2\text{T}-\text{PEt}_2)_6]$	2b
$[\text{W}_6\text{S}_8(3\text{T}-\text{PPh}_2)_6]$	3a
$[\text{W}_6\text{S}_8(3\text{T}-\text{PEt}_2)_6]$	3b
$[\text{W}_6\text{S}_8((2\text{T})_3\text{P})_6]$	4
$[\text{W}_6\text{S}_8(2\text{EDOT}-\text{PEt}_2)_6]$	5

and six of them have been characterized by X-ray diffraction on single crystals. In this investigation, new phosphino–thiophene ligands have been also prepared and characterized. The electropolymerization of some of these hybrid organic–inorganic clusters has been studied.

Experimental Section

General Procedures. All manipulations were performed with standard air-free techniques in an argon-filled glovebox and using standard Schlenk equipment, unless otherwise noted. Solvents were distilled from appropriate drying agents and degassed prior to use.

$[\text{W}_6\text{S}_8(\text{tbp})_6]$ (tbp = 4-*tert*-butylpyridine) and $[\text{W}_6\text{S}_8(\text{PEt}_3)_6]$ were synthesized as previously reported.⁴⁰ 5-Bromothiophene, 5-bromobithiophene, terthiophene and EDOT were purchased from Aldrich and used as received, as well as *n*-butyllithium (1.6 M in hexanes), diisopropylamine, PPh_2Cl , PEt_2Cl , and PBr_3 . 2EDOT was synthesized by the method reported in the literature.⁴¹

^1H and ^{31}P NMR spectra were recorded on Varian Inova 400 and Varian Mercury 300 spectrometers at room temperature. ^1H spectra were internally referenced to residual protonated solvent peaks. The ^{31}P spectra were ^1H decoupled, and 85% H_3PO_4 was used as an external standard.

Elemental analyses (C, H, N, P) were performed by Robertson Microlit Laboratories, Inc., at Madison, NJ.

UV–vis spectra were recorded with a Perkin-Elmer Lambda 2 spectrometer. Measurements were made on dichloromethane solutions except for **4**, for which benzonitrile was used. Concentrations of $1.5 \times 10^{-5} \text{ mol}\cdot\text{L}^{-1}$ for the clusters and $5 \times 10^{-5} \text{ mol}\cdot\text{L}^{-1}$ for the ligands were used.

Cyclic voltammetry (CV) experiments were performed with an EG&G PAR 273A potentiostat using a Pt disk working electrode, a large area Pt wire counter electrode and a Ag/AgCl reference electrode. The electrolytic media was a $0.1 \text{ mol}\cdot\text{L}^{-1}$ dichloromethane solution of (*n*-Bu₄N)PF₆ except for **4**, for which benzonitrile was used. The concentration used for the clusters was $10^{-3} \text{ mol}\cdot\text{L}^{-1}$ and $5 \times 10^{-2} \text{ mol}\cdot\text{L}^{-1}$ for the ligands. All experiments were performed at room temperature under a N₂ atmosphere.

Synthesis of the Clusters. $[\text{W}_6\text{S}_8(\text{T}-\text{PPh}_2)_6]$ (**1a**). A benzene solution (15 mL) containing $[\text{W}_6\text{S}_8(\text{tbp})_6]$ (80 mg, 0.037 mmol) and T–PPh₂ (180 mg, 0.67 mmol) was heated at 60 °C for 5 days. After cooling down, brown crystals were obtained. The product was recovered by filtration followed by washing with diethyl ether and drying under vacuum.

Yield (based on $[\text{W}_6\text{S}_8(\text{tbp})_6]$): 60 mg, 0.020 mmol (55%). $^{31}\text{P}\{^1\text{H}\}$ NMR (C₆D₆): δ (ppm) –13.6 (s). Anal. Calcd for

$\text{C}_9\text{H}_7\text{P}_6\text{S}_{14}\text{W}_6 + \text{C}_6\text{H}_6$: C, 40.20; H, 2.78; P, 6.10. Found: C, 40.12; H, 2.84; P, 5.70.

$[\text{W}_6\text{S}_8(\text{T}-\text{PEt}_2)_6]$ (**1b**). A benzene solution (15 mL) containing $[\text{W}_6\text{S}_8(\text{tbp})_6]$ (100 mg, 0.046 mmol) and T–PEt₂ (127 mg, 0.74 mmol) was heated at 70 °C with stirring for 4 days. After cooling and evaporation of half of the solvent, dark red crystals were obtained, which were then washed with diethyl ether and dried under vacuum.

Yield (based on $[\text{W}_6\text{S}_8(\text{tbp})_6]$): 100 mg, 0.042 mmol (91%). ^1H NMR (CDCl₃): δ (ppm) 7.82–7.79 (dd, 1H, $J = 3.2, 5.6$ Hz); 7.53–7.52 (d, 1H, $J = 4.8$ Hz); 7.06–7.04 (dd, 1H, $J = 4, 4$ Hz); 2.27–2.20 (m, 4H, Et); 1.16–1.09 (m, 6H, Et). $^{31}\text{P}\{^1\text{H}\}$ NMR (CDCl₃): δ (ppm) –21.2 (s); (C₆D₆): δ (ppm) –19.7 (s). Anal. Calcd for $\text{C}_{48}\text{H}_{78}\text{P}_6\text{S}_{14}\text{W}_6 + 2(\text{C}_6\text{H}_6)$: C, 28.27; H, 3.56; P, 7.29. Found: C, 27.85; H, 3.46; P, 7.34.

$[\text{W}_6\text{S}_8(2\text{T}-\text{PPh}_2)_6]$ (**2a**). A benzene solution (10 mL) containing $[\text{W}_6\text{S}_8(\text{tbp})_6]$ (50 mg, 0.023 mmol) and 2T–PPh₂ (100 mg, 0.29 mmol) was heated at 70 °C with stirring for 7 days. After cooling, the solution was filtered to remove a slight precipitate and diethyl ether was slowly diffused on it. Dark brown crystals were obtained, which were then washed with diethyl ether and dried under vacuum.

Yield (based on $[\text{W}_6\text{S}_8(\text{tbp})_6]$): 60 mg, 0.017 mmol (75%). Brown crystals of better crystalline quality were obtained by concentrating by half a benzene solution of the cluster by slow evaporation of the solvent in air. The latter were thus used for the single-crystal X-ray diffraction study. ^1H NMR (CDCl₃): δ (ppm) 7.59–7.57 (dd, 1H, $J = 3.6, 6.4$ Hz); 7.16–7.14 (dd, 1H, $J = 0.8$ Hz, 4.8); 6.96–6.95 (dd, 1H, $J = 0.8, 4.4$ Hz); 6.91–6.89 (ddd, 1H, $J = 0.8, 3.6, 4.8$ Hz); 6.85–6.84 (dd, 1H, $J = 0.8, 2.8$ Hz); 7.51–7.47 (m, 4H, Ph); 7.27–7.23 (m, 2H, Ph); 7.12–7.08 (m, 4H, Ph). $^{31}\text{P}\{^1\text{H}\}$ NMR (CDCl₃): δ (ppm) –14.3 (s). Anal. Calcd for $\text{C}_{120}\text{H}_{90}\text{P}_6\text{S}_{20}\text{W}_6$: C, 41.63; H, 2.62; P, 5.37. Found: C, 41.03; H, 2.31; P, 4.72.

$[\text{W}_6\text{S}_8(2\text{T}-\text{PEt}_2)_6]$ (**2b**). A benzene solution (15 mL) containing $[\text{W}_6\text{S}_8(\text{tbp})_6]$ (70 mg, 0.032 mmol) and 2T–PEt₂ (130 mg, 0.51 mmol) was heated at 70 °C with stirring for 4 days. After cooling, the solution was filtered to remove a slight precipitate and ether was diffused on it. Dark brown platelet crystals were obtained, which were then washed with diethyl ether and dried under vacuum.

Yield (based on $[\text{W}_6\text{S}_8(\text{tbp})_6]$): 65 mg, 0.022 mmol (70%). ^1H NMR (CD₂Cl₂): δ (ppm) 7.61–7.59 (dd, 1H, $J = 3.6, 5.6$ Hz); 7.25–7.23 (dd, 1H, $J = 1.2, 5.2$ Hz); 7.17–7.15 (dd, 1H, $J = 1.2, 3.6$ Hz); 7.14–7.13 (dd, 1H, $J = 1.2, 3.6$ Hz); 7.02–7.00 (dd, 1H, $J = 4, 5.2$ Hz); 2.26–2.19 (m, 4H, Et); 1.18–1.11 (m, 6H, Et). $^{31}\text{P}\{^1\text{H}\}$ NMR (C₆D₆): δ (ppm) –18.5 (s). Anal. Calcd for $\text{C}_{72}\text{H}_{90}\text{P}_6\text{S}_{20}\text{W}_6$: C, 29.97; H, 3.14; N, 0. Found: C, 29.81; H, 2.93; N, <0.02.

$[\text{W}_6\text{S}_8(3\text{T}-\text{PPh}_2)_6]$ (**3a**). A benzene solution (15 mL) containing $[\text{W}_6\text{S}_8(\text{tbp})_6]$ (80 mg, 0.037 mmol) and 3T–PPh₂ (300 mg, 0.69 mmol) was heated at 60 °C with stirring for 8 days. A brown–yellow precipitate appeared in the solution. The solid was recovered by filtration following by washing with diethyl ether and drying under vacuum. Yield (based on $[\text{W}_6\text{S}_8(\text{tbp})_6]$): 90 mg, 0.023 mmol (62%). Due to the very low solubility of this compound, no crystals were obtained.

^1H NMR (CDCl₃): δ (ppm) 7.57–7.55 (dd, 1H, $J = 4, 6.4$ Hz); 7.18–7.16 (dd, 1H, $J = 1.2, 5.2$ Hz); 7.07–7.06 (dd, 1H, $J = 1.2, 3.6$ Hz); 6.96–6.94 (dd, 1H, $J = 3.6, 4.8$ Hz); 6.93–6.91 (d, 1H, $J = 2.8$ Hz); 6.86–6.85 (dd, 1H, $J = 1.6, 3.6$ Hz); 6.84–6.83 (d, 1H, $J = 3.6$ Hz); 7.54–7.48 (m, 4H, Ph); 7.29–7.25 (m, 2H, Ph); 7.13–7.10 (m, 4H, Ph). $^{31}\text{P}\{^1\text{H}\}$ NMR (CDCl₃): δ (ppm) –14.0 (s). Anal. Calcd for $\text{C}_{144}\text{H}_{102}\text{P}_6\text{S}_{26}\text{W}_6$: C, 43.73; H, 2.60; P, 4.70. Found: C, 42.67; H, 2.48; P, 3.84.

(40) Venkataraman, D.; Rayburn, L.; Hill, L.; Jin, S.; Malik, A.-S.; Tumeau, K.; DiSalvo, F. J. *Inorg. Chem.* **1999**, *38*, 828–830.

(41) Leriche, P.; Turbiez, M.; Monroche, V.; Frere, P.; Blanchard, P.; Skabara, P. J.; Roncali, J. *Tetrahedron Lett.* **2003**, *44*, 649–652.

Table 1. Crystal Data and Structure Refinement for **1a**·(C₆H₆), **1b**·(C₆H₆)₂, **2a**·(C₆H₆)₆, **2b**, **3b**, and **4**·(C₇H₅N)₄

	compound					
	[W ₆ S ₈ (T–PPh ₂) ₆] ·(C ₆ H ₆)	[W ₆ S ₈ (T–PEt ₂) ₆] ·(C ₆ H ₆) ₂	[W ₆ S ₈ (2T–PPh ₂) ₆] ·(C ₆ H ₆) ₆	[W ₆ S ₈ (2T–PEt ₂) ₆]	[W ₆ S ₈ (3T–PEt ₂) ₆]	[W ₆ S ₈ ((2T) ₃ P) ₆] ·(C ₇ H ₅ N) ₄
label	1a ·(C ₆ H ₆)	1b ·(C ₆ H ₆) ₂	2a ·(C ₆ H ₆) ₆	2b	3b	4 ·(C ₇ H ₅ N) ₄
chemical formula	C ₁₀₂ H ₈₄ P ₆ S ₁₄ W ₆	C ₆₀ H ₉₀ P ₆ S ₁₄ W ₆	C ₁₅₆ H ₁₂₄ P ₆ S ₂₀ W ₆	C ₇₂ H ₉₀ P ₆ S ₂₀ W ₆	C ₉₆ H ₁₀₂ P ₆ S ₂₆ W ₆	C ₂₀₀ H ₁₃₀ N ₈ P ₆ S ₄₄ W ₆
fw	3047.54	2549.16	3928.82	2885.56	3378.26	5345.07
cryst syst	triclinic	triclinic	triclinic	triclinic	monoclinic	triclinic
space group	<i>P</i> $\bar{1}$	<i>P</i> $\bar{1}$	<i>P</i> $\bar{1}$	<i>P</i> $\bar{1}$	<i>P</i> 2 ₁ / <i>c</i>	<i>P</i> $\bar{1}$
<i>a</i> , Å	14.0505(6)	13.2939(8)	13.9793(9)	11.5202(10)	18.9053(12)	17.6565(8)
<i>b</i> , Å	14.4887(7)	13.3562(9)	16.2266(10)	14.0861(12)	12.4825(8)	17.8491(10)
<i>c</i> , Å	15.7381(7)	13.3814(9)	17.7880(11)	15.7759(14)	23.4470(15)	18.7334(11)
α , deg	63.2540(10)	82.066(3)	115.720(1)	69.288(4)	90	64.432(2)
β , deg	66.0090(10)	67.474(3)	91.078(2)	68.914(4)	106.183(2)	75.920(2)
γ , deg	63.8300(10)	60.824(2)	91.837(2)	71.871(3)	90	70.635(2)
<i>V</i> , Å ³	2479.7(2)	1912.7(2)	3630.9(4)	2184.1(3)	5313.9(6)	4989.5(5)
<i>Z</i>	1	1	1	1	2	1
ρ_{calc} , g/cm ³	2.041	2.213	1.797	2.194	2.111	1.779
μ , mm ⁻¹	7.369	9.529	5.138	8.497	7.116	4.009
reflns collected	62 580	76 491	125 608	51 643	65 636	85 132
indep reflns	21 280	18 193	32 665	16 027	13 696	17 579
<i>R</i> _{int}	0.0417	0.0354	0.0830	0.0398	0.0616	0.0540
reflns <i>I</i> > 2 σ (<i>I</i>)	16 527	13 916	24 558	11 293	9272	12 738
params	631	388	830	469	605	1174
GOF on <i>F</i> ²	0.940	1.082	1.091	1.019	0.980	1.020
<i>R</i> ₁ ^a / <i>R</i> ₂ ^b (<i>I</i> > 2 σ (<i>I</i>))	0.0430/0.1025	0.0269/0.0496	0.0955/0.2015	0.0336/0.0719	0.0355/0.0644	0.0349/0.0772
<i>R</i> ₁ ^a / <i>R</i> ₂ ^b (all)	0.0658/0.1247	0.0444/0.0522	0.1275/0.2195	0.0681/0.0848	0.0728/0.0723	0.0627/0.0863

^a $R_1 = \sum \text{abs}(\text{abs}(F_o) - \text{abs}(F_c)) / \sum \text{abs}(F_o)$. ^b $R_2 = (\sum [w(F_o^2 - F_c^2)] / \sum [w(F_o^2)])^{0.5}$.

[W₆S₈(3T–PEt₂)₆] (**3b**). A benzene solution (12 mL) containing [W₆S₈(tbp)₆] (70 mg, 0.032 mmol) and 3T–PEt₂ (200 mg, 0.60 mmol) was heated at 60 °C for 6 days. By cooling, brown-yellow crystals formed in the solution. After filtration, the product was washed with benzene and diethyl ether and then dried under vacuum.

Yield (based on [W₆S₈(tbp)₆]): 90 mg, 0.026 mmol (82%). Anal. Calcd for C₉₆H₁₀₂P₆S₂₆W₆: C, 34.13; H, 3.04. Found: C, 34.99; H, 2.92.

[W₆S₈((2T)₃P)₆] (**4**). A benzene solution (15 mL) containing [W₆S₈(tbp)₆] (50 mg, 0.023 mmol) and (2T)₃P (220 mg, 0.42 mmol) was heated at 60 °C for 10 days. By cooling, brown-red crystals formed in the solution. After filtration, the product was washed with benzene and diethyl ether and then dried under vacuum. Yield (based on [W₆S₈(tbp)₆]): 60 mg, 0.013 mmol (58%). Recrystallization in benzonitrile gave red prism-shaped crystals which were used for the single-crystal X-ray diffraction analysis. These crystals lose solvent very rapidly when exposed to air.

¹H NMR (CD₂Cl₂): δ (ppm) 7.57–7.54 (dd, 1H, *J* = 4, 7.2 Hz); 7.18–7.16 (dd, 1H, *J* = 1.2, 5.2 Hz); 6.99–6.97 (dd, 1H, *J* = 1.2, 3.6 Hz); 6.91–6.90 (dd, 1H, *J* = 1.2, 2.8 Hz); 6.90–6.87 (dd, 1H, *J* = 3.6, 5.2 Hz). ³¹P{¹H} NMR (C₆D₆): δ (ppm) –35.2 (s). Anal. Calcd for C₁₄₄H₉₀P₆S₄₄W₆: C, 38.26; H, 2.01; N, 0. Found: C, 38.46; H, 1.88; N, <0.02.

[W₆S₈(2EDOT–PEt₂)₆] (**5**). A benzene solution (15 mL) containing [W₆S₈(tbp)₆] (50 mg, 0.023 mmol) and 2EDOT–PEt₂ (170 mg, 0.46 mmol) was heated at 60 °C for 10 days. Orange-red platelet-shaped crystals formed in the solution. After filtration, the product was washed with benzene and diethyl ether and then dried under vacuum. Yield (based on [W₆S₈(tbp)₆]): 70 mg, 0.020 mmol (85%). These crystals lose solvent very rapidly when exposed to air. The crystalline quality was not high enough to solve the crystal structure by X-ray diffraction.

Anal. Calcd for C₉₆H₁₁₄P₆S₂₀W₆O₂₄: C, 32.19; H, 3.21; N, 0. Found: C, 32.55; H, 2.89; N, <0.02.

X-ray Structure Determination. Single crystals suitable for X-ray analyses were obtained for clusters **1a–2b**, **3b**, and **4** (as

described in the synthesis section). Crystals were mounted on thin nylon loops using polybutene oil and immediately cooled to 173 K in a cold stream of nitrogen. Single-crystal diffraction data were collected on a Bruker SMART system with a CCD detector using Mo K α radiation ($\lambda = 0.71073$ Å). The cell parameters were initially determined using more than 50 reflections. The data were integrated using *SAIN*T⁴² software, and empirical absorption corrections were determined and applied using the *SADABS*⁴³ program. The structures were solved by direct methods using *SHELXS-86* and refined by the full matrix least-squares method on *F*², using the *SHELXL-97* software package.⁴⁴ In all structures, hydrogen atoms were introduced at calculated positions and not refined (riding model). Details of crystal data and structure refinements are summarized in Table 1.

For **1a**, all non-hydrogen atoms were refined with anisotropic thermal parameters. In two of the three independent T–PPh₂ ligands, the thiophene ring is disordered with the two phenyl groups. This disorder is due to the similar geometry of these two moieties.

For **2a**, all non-hydrogen atoms were refined with anisotropic thermal parameters except disordered carbon and sulfur atoms, which were refined isotropically. For one of the three independent bithiophene groups, the sulfur atom of the terminal ring is disordered over two positions sharing the same site with a carbon atom. The hydrogen atom has not been introduced on these disordered carbon atoms. The corresponding occupancy levels have been refined at 0.53/0.47. Two of the six independent phenyl groups present an orientation disorder by rotation around the P–C bond.

For **1b** and **2b**, all non-hydrogen atoms were refined with anisotropic thermal parameters.

For **3b**, all non-hydrogen atoms were refined with anisotropic thermal parameters. For two of the three independent terthiophene

(42) *SAIN*T Plus: Software for the CCD Detector System; Bruker Analytical X-Ray Instruments, Inc.: Madison, WI, 1999.

(43) Sheldrick, G. M. *SADABS*; University of Göttingen: Göttingen, Germany, 1999.

(44) Sheldrick, G. M. *SHELX-97*; University of Göttingen, Göttingen, Germany, 1997.

groups, the sulfur atom of the terminal thiophene ring is disordered over two positions sharing the same site with a carbon atom. The corresponding occupancy levels have been refined and then fixed at 0.5/0.5 for one atomic site and 0.7/0.3 for the other. For the two different thiophene rings, the hydrogen atom has been introduced on only one of the two disordered sulfur/carbon atoms.

For **4**, all non-hydrogen atoms were refined with anisotropic thermal parameters except three carbon atoms of thiophene rings which were refined isotropically.

Results and Discussion

Syntheses. Ligands. The experimental information for the ligand syntheses is reported in the Supporting Information. The phosphino–thiophene ligands T–PPh₂,⁴⁵ 2T–PPh₂,⁴⁶ and 3T–PPh₂⁴⁷ were synthesized by modification of reported procedures. The lithiation of the thiophene oligomers (T, 2T, and 3T) was realized by reaction with *n*-butyl-lithium at low temperature. Next, the addition of the chlorophosphine PPh₂-Cl, led to the desired thiophene–phosphine derivatives. To improve the solubility of the functionalized clusters, replacement of the phenyl groups by ethyl groups was investigated. The ligands *n*T–PEt₂ (*n* = 1, 2, 3) were then prepared by the same reaction using PEt₂Cl as the reactant. Moreover, the ligands *n*T–PEt₂ were found to be more reactive toward the coordination of the clusters compared with the *n*T–PPh₂ ligands (see below).

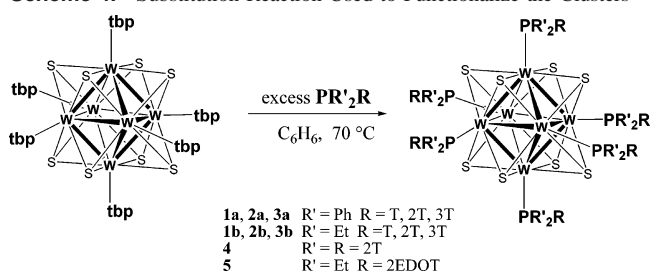
(2T)₃P was synthesized by reacting PBr₃ with the lithiated bithiophene. This ligand bearing three bithiophene moieties is expected to promote the polymerization of the corresponding functionalized cluster. Indeed, this new molecule itself can also be considered to prepare purely organic polymer.

To lower the polymerization potential of the ligand, three EDOT derivatives formulated EDOT–PPh₂ and 2EDOT–PR₂ (R = Ph, Et) were synthesized by using the same procedure. Indeed, the EDOT moiety is known to oxidize at lower potential compared with thiophene. The synthesis of (EDOT)_{*n*}PPh_{3–*n*} (*n* = 1–3) has already been reported,⁴⁸ but to our knowledge the 2EDOT–PR₂ ligands are the first phosphino–bisEDOT derivatives. Indeed, whereas the use of thiophene oligomers functionalized with coordinative groups has been studied, examples of EDOT derivatives bearing coordinating groups are quite rare.

Clusters. Large amounts of [W₆S₈(tbp)₆] (tbp = 4-*tert*-butylpyridine) can be easily synthesized in high yield.⁴⁰ This cluster was thus used as the precursor cluster for the functionalization reactions. In this compound, the six tbp ligands coordinate each of the six tungsten atoms. The replacement of these six labile ligands by phosphine derivatives, which are known to be more strongly bonded ligands, has been already well studied.^{30–35}

By heating a benzene solution of the [W₆S₈(tbp)₆] cluster and the phosphine ligand, the corresponding hexasubstituted

Scheme 4. Substitution Reaction Used to Functionalize the Clusters^a



^a Note: tbp = 4-*tert*-butylpyridine; PR'₂R = thiophene–phosphine derivatives.

phosphine-coordinated clusters were obtained (Scheme 4). Note that other solvents were used in place of the benzene but with no success. Most of the time, a large excess of the ligand was employed to promote the complete exchange of the six terminal ligands. The solution turned progressively red to brown as the reaction proceeded. The reactions were usually monitored by ¹H and ³¹P NMR spectroscopy, which showed that the reactions were complete within several days (only uncoordinated tbp ligands are detected). The products were usually recovered in crystalline form in high yield because most of the clusters seem to precipitate once the hexasubstitution was achieved. A shorter reaction time was observed by NMR for the *n*T–PEt₂ ligands compared with the *n*T–PPh₂ ones. The reaction time was also longer as the oligomer length increased.

Reactions with the *n*EDOT–PPh₂ (*n* = 1, 2) ligands led systematically to brown precipitates, and no solvent could be found to solubilize them. The solubility of the EDOT derivatives was found to be significantly lower compared with that of their thiophene analogues. Even after 10 days of reaction, the ³¹P NMR spectra showed multiple peaks corresponding to a mixture of partially substituted clusters. We can even suggest that the cluster precipitates before the hexasubstitution thus leading to the formation of an amorphous solid. By increasing the reactivity and the solubility with 2EDOT–PEt₂, crystals of the corresponding cluster (**5**) were obtained. Unfortunately, the solubility of the latter was not good enough for further solution studies. The reactivity of (2T)₃P is quite similar to that of the EDOT derivatives, and a long reaction time was needed to obtain the corresponding cluster (**4**). Solubility was probably also the issue in this case.

The functionalized clusters (**1–5**) were characterized by elemental analysis, NMR when soluble, and for some of them by single-crystal X-ray diffraction (**1a–2b**, **3b**, and **4**). Due to the symmetry of the hexasubstituted cluster, a singlet is observed in the ³¹P NMR spectra.⁴⁹ This signal is downfield shifted compared with that of the corresponding free ligand. For example, the spectrum of [W₆S₈(T–PEt₂)₆] displays a single resonance at –19.7 ppm whereas the signal of the corresponding free ligand is at –25.7 ppm (in C₆D₆). Along the [W₆S₈(*n*T–PR₂)₆] (R = Ph, Et) series, a downfield shift is observed for the ³¹P signal by increasing the thiophene chain length and an upfield shift is observed by replacement

(45) Jain, V. K.; Clark, H. C.; Jain, L. *Indian J. Chem.* **2001**, *40A*, 135–143.

(46) Myrex, R. D.; Colbert, C. S.; Gray, G. M. *Organometallics* **2004**, *23*, 409–415.

(47) Clot, O.; Wolf, M. O.; Patrick, B. O. *J. Am. Chem. Soc.* **2001**, *123*, 9963–9973.

(48) Chahma, M.; Myles, D. J. T.; Hicks, R. G. *Can. J. Chem.* **2005**, *83*, 150–155.

(49) Jin, S.; Adamchuk, J.; Xiang, B.; DiSalvo, F. J. *J. Am. Chem. Soc.* **2002**, *124*, 9229–9240.

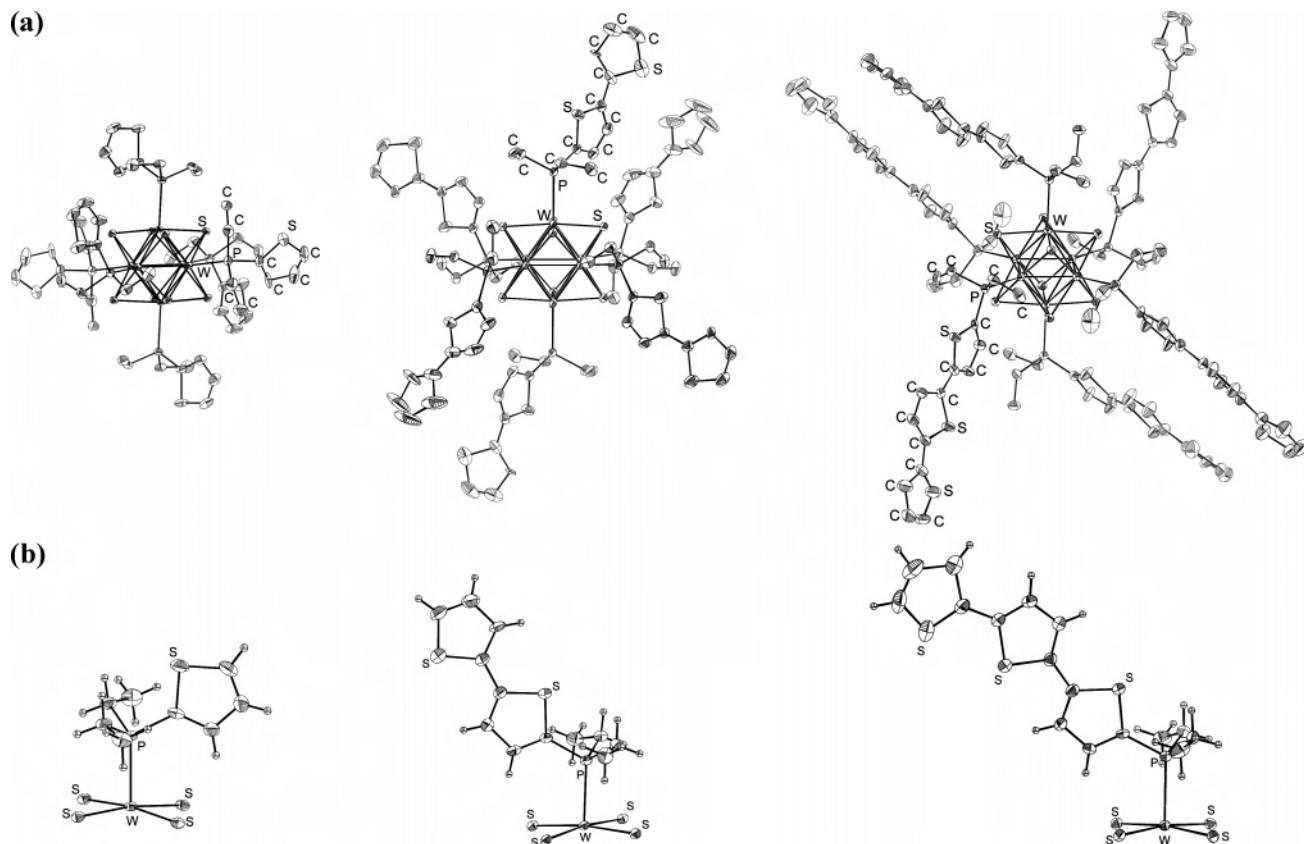


Figure 1. (a). Molecular structures of **1b**, **2b**, and **3b**. Three of the six ligands are in gray for better clarity. Hydrogen atoms are omitted. The thermal ellipsoids are at the 50% probability level. (b) Coordination geometry of the ligand in **1b**, **2b**, and **3b**. The other two crystallographically independent ligands present a similar coordination mode. Nonlabeled atoms are carbon or hydrogen atoms. The thermal ellipsoids are at the 50% probability level.

of the phenyl groups by ethyl groups. These tendencies are also observed for the corresponding uncoordinated ligands.

Crystal Structures. The crystal structures of clusters **1a–2b**, **3b**, and **4** have been solved by single-crystal X-ray diffraction. All the clusters crystallize in the $P\bar{1}$ triclinic space group except cluster **3b**, which crystallizes in the $P2_1/c$ monoclinic space group. For clusters **1a–2a** and **4**, solvent molecules are included in the structures that lead to the formulas $[W_6S_8(T-PPh_2)_6] \cdot (C_6H_6)$, $[W_6S_8(T-PEt_2)_6] \cdot (C_6H_6)_2$, $[W_6S_8(2T-PPh_2)_6] \cdot (C_6H_6)_6$, and $[W_6S_8((2T)_3P)_6] \cdot (C_7H_5N)_4$, respectively.

The molecular structures of the clusters are shown in Figures 1a and 2a. In all cases, the cluster sits on an inversion center so half of the cluster is crystallographically independent. Selected bond lengths and angles are listed in Table 2. For all clusters, the $[W_6S_8]$ core presents a classical geometry with W–W, W–S, and W–P bonds comparable to those already observed for other neutral (20 metal-based electrons) octahedral tungsten clusters coordinated by phosphorus ligands.^{30–35} As expected, the six thiophene–phosphine ligands are coordinated to the six W atoms via the phosphorus atom (Figures 1b and 2b). It confirms unambiguously the complete replacement of the pyridine ligands in the six apical positions by the thiophene derivatives.

For some of the clusters, the ligands are disordered. Indeed, due to their similar geometries, the thiophene ring is disordered with the phenyl groups for the ligand T–PPh₂ in the cluster **1a**. Moreover, two thiophene groups can be in

syn or anti conformation, so an average of these two conformations can be observed by X-ray analysis. This disorder is observed in **2a** for one bithiophene group and in **3b** for the terminal ring of two terthiophene moieties. No disorder is observed in **2b** and **4**; all the ligands are in anti conformation in **2b**, and on the nine independent bithiophene groups in **4**, five are in anti conformation and four are in syn conformation.

When not disordered, the thiophene rings present a classical geometry for a neutral state with C–C and C–S bonds in common range and similar to those observed in complexes of T–PPh₂ reported in the literature.^{50–53} The molecular structures of two complexes of 3T–PPh₂ formulated $(3T-PPh_2)AuCl$ ⁵⁴ and $(3T-PPh_2)_2PdCl_2$ ⁵⁵ have been reported. In these complexes, the geometry of the ligand is comparable to that of 3T–PEt₂ in **3b**.

It is worth noting that we have obtained the crystal structure of functionalized clusters bearing either 6 (**1a,b**), 12 (**2a,b**), 18 (**3b**), or 36 (**4**) thiophene units. The latter two represent the largest number of thiophene groups with free

(50) Dick, D. G.; Stephan, D. W. *Can. J. Chem.* **1986**, *64*, 1870–1875.

(51) King, J. D.; Monari, M.; Nordlander, E. *J. Organomet. Chem.* **1999**, *573*, 272–278.

(52) Cauzzi, D.; Graiff, C.; Massera, C.; Predieri, G.; Tiripicchio, A. *Inorg. Chim. Acta* **2000**, *300*, 471–476.

(53) Deeming, A. J.; Jayasuriya, S. N.; Arce, A. J.; De Sanctis, Y. *Organometallics* **1996**, *15*, 786–793.

(54) Scott, T. L.; Wolf, M. O.; Patrick, B. O. *Inorg. Chem.* **2005**, *44*, 620–627.

(55) Scott, T. L.; Wolf, M. O.; Lam, A. *Dalton Trans.* **2005**, 652–653.

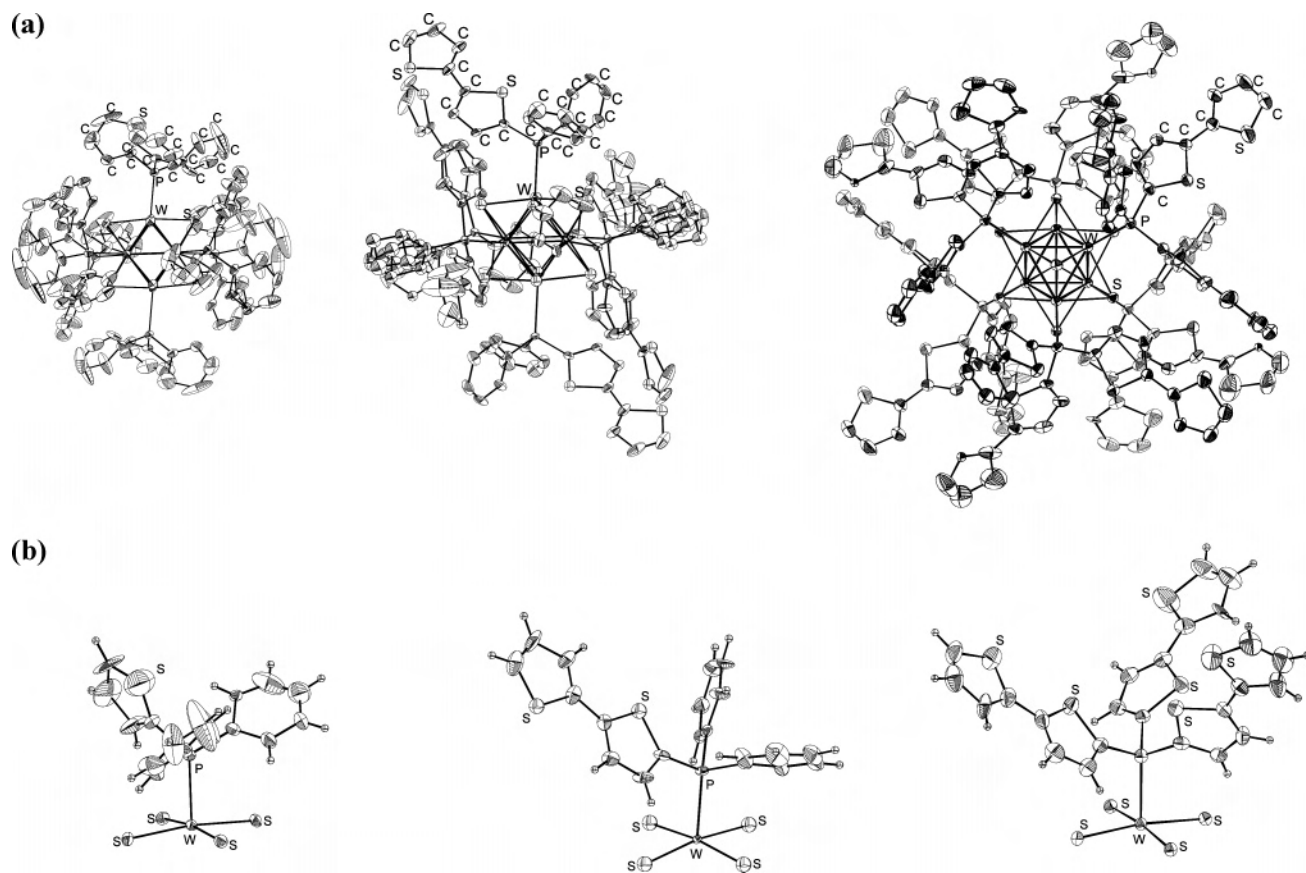


Figure 2. (a) Molecular structures of **1a**, **2a**, and **4**. Three of the six ligands are in gray for better clarity. Hydrogen atoms are omitted. The thermal ellipsoids are at the 50% probability level. (b) Coordination geometry of the ligand in **1a**, **2a**, and **4**. The other two crystallographically independent ligands present a similar coordination mode. Nonlabeled atoms are carbon or hydrogen atoms. The thermal ellipsoids are at the 50% probability level.

Table 2. Selected Bonds Lengths (Å) and Angles (deg) in Clusters **1a–2b**, **3b**, and **4**

	compound					
	[W ₆ S ₈ (T–PPh ₂) ₆] (1a)	[W ₆ S ₈ (T–PEt ₂) ₆] (1b)	[W ₆ S ₈ (2T–PPh ₂) ₆] (2a)	[W ₆ S ₈ (2T–PEt ₂) ₆] (2b)	[W ₆ S ₈ (3T–PEt ₂) ₆] (3b)	[W ₆ S ₈ ((2T) ₃ P) ₆] (4)
	W–W					
mean	2.6781(25)	2.6741(43)	2.6833(54)	2.6770(68)	2.6777(56)	2.6758(50)
range	2.6748(3)– 2.6824(3)	2.6708(2)– 2.6825(2)	2.6739(4)– 2.6910(4)	2.6664(3)– 2.6860(3)	2.6698(3)– 2.6867(3)	2.6704(4)– 2.6842(4)
	W–S					
mean	2.455(12)	2.451(8)	2.425(8)	2.461(9)	2.454(9)	2.453(10)
range	2.4282(13)– 2.4643(13)	2.4373(6)– 2.4623(6)	2.411(2)– 2.445(2)	2.4475(11)– 2.4773(12)	2.4417(13)– 2.4667(13)	2.4335(15)– 2.4659(15)
	W–P					
	2.5476(14)	2.5464(6)	2.574(2)	2.5305(13)	2.5522(13)	2.5289(16)
	2.5408(14)	2.5467(6)	2.555(2)	2.5423(12)	2.5311(14)	2.5314(15)
	2.5562(13)	2.5373(7)	2.544(2)	2.5511(12)	2.5689(14)	2.5279(16)
	W–W–W					
range ^a	59.857(7)– 60.138(8)	59.841(5)– 60.276(6)	59.659(11)– 60.289(11)	59.678(8)– 60.291(9)	59.718(8)– 60.344(8)	59.763(9)– 60.211(9)
range ^b	89.775(8)– 90.225(8)	89.844(7)– 90.156(6)	89.683(13)– 90.317(13)	89.752(9)– 90.248(9)	89.588(9)– 90.412(9)	89.944(11)– 90.056(11)

^a W–W–W angles within the equatorial squares; the mean value is automatically 90° because the clusters are centered on an inversion center. ^b W–W–W angles within the triangular faces; the mean value is 60° by geometry.

α positions, incorporated in a single crystallized molecule. To our knowledge, the largest known species so far were Mn₁₂ single-molecule magnets with 16⁹ and 17¹⁰ mono-thiophenes carboxylates.

UV–Vis Study. Ligands. The absorption spectra of the ligands nT –PEt₂ ($n = 1, 2, 3$) and (2T)₃P in solution are

reported in Figure 3. The corresponding band values are listed in Table 3.

The most intense band observed in the spectra corresponds to the $\pi \rightarrow \pi^*$ transition of the thiophene moiety of the ligands. Along the nT –PEt₂ ($n = 1, 2, 3$) series, this absorbance band is red-shifted as the oligomer length

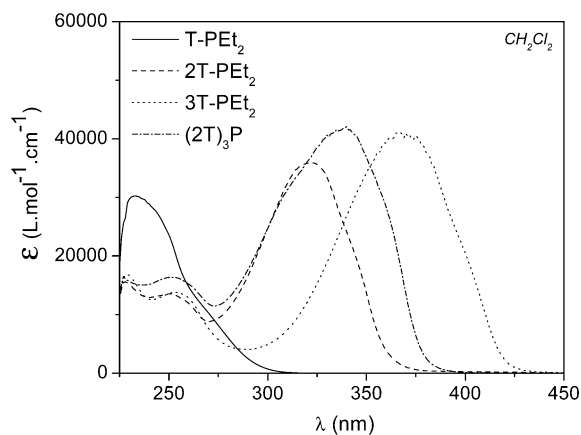


Figure 3. UV-vis spectra of the ligands $nT-PEt_2$ ($n = 1, 2, 3$) and $(2T)_3P$ in CH_2Cl_2 .

Table 3. Absorption Data of the Ligands^a

ligands				
T-PEt ₂	2T-PEt ₂	3T-PEt ₂	(2T) ₃ P	
233 (30)	228 (15)	229 (17)	227 (16)	
	253 (13)	255 (14)	252 (16)	
	321 (36)	368 (41)	338 (42)	343 (100) ^b

^a In CH_2Cl_2 , unless otherwise noted, and with units λ_{max}/nm ($\epsilon_{max}/10^3 \cdot L \cdot mol^{-1} \cdot cm^{-1}$). ^b Values in benzonitrile

increases (see Table 3). The shift between two ligands decreases progressively as the oligomer length increases. This phenomenon has been already reported for the phenyl derivatives (T-PPh₂ 265 nm, 2T-PPh₂ 330 nm, and 3T-PPh₂ 374 nm),⁵⁶ and it is also known for the unsubstituted oligomers (T 231 nm, 2T 303 nm, and 3T 354 nm).⁵⁷ The incorporation of the phosphine group on the thiophene backbone induces a red shift in the absorbance band, which is more pronounced for the phenyl series compared with the ethyl one. This shift has been attributed to the stabilization of the lowest unoccupied molecular orbital (LUMO) by a bonding interaction between the phosphorus atom and the thienyl π system.⁵⁶ Concerning the bithiophene derivatives, $(2T)_3P$ presents the larger red shift. The following wavelength evolution can be then established: $2T < 2T-PEt_2 < 2T-PPh_2 < (2T)_3P$.

For all the ligands (except for T-PEt₂ where the band is not well resolved), two bands are systematically observed around 230 and 250 nm. The band at 250 nm has been attributed to the $n(P) \rightarrow \pi^*(T)$ transition.⁵⁶

Clusters. The absorption spectra of the cluster $[W_6S_8(nT-PEt_2)_6]$ and $[W_6S_8(nT-PPh_2)_6]$ ($n = 1, 2, 3$) series, in solution, from 225 to 600 nm, are reported in Figures 4 and 5, respectively. The spectra recorded from 225 to 1000 nm are reported in the Supporting Information. The corresponding band values are listed in Table 4.

Six absorption bands are observed in the $[W_6S_8(PEt_3)_6]$ spectra. It has been suggested that the band at 882 nm corresponds to the LUMO-HOMO (HOMO = highest occupied molecular orbital) transition of the cluster.² In

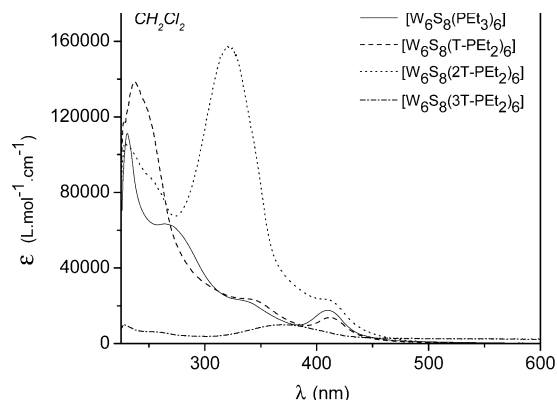


Figure 4. UV-vis spectra of clusters $[W_6S_8(nT-PEt_2)_6]$ ($n = 1, 2, 3$) and $[W_6S_8(PEt_3)_6]$ in CH_2Cl_2 .

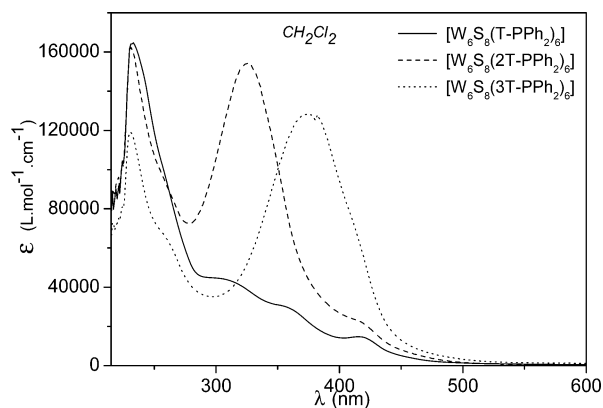


Figure 5. UV-vis spectra of clusters $[W_6S_8(nT-PPh_2)_6]$ ($n = 1, 2, 3$) in CH_2Cl_2 .

Table 4. Absorption Data of the Clusters^a

clusters			
$[W_6S_8(PEt_3)_6]$	$[W_6S_8(T-PEt_2)_6]$	$[W_6S_8(2T-PEt_2)_6]$	$[W_6S_8(3T-PEt_2)_6]$ ^b
231 (111)	238 (139)	229 (106)	228
266 (63)		256 (84) sh	258 sh
338 (22) sh	344 (23)	320 (157)	374
411 (17)	412 (14)	411 (23)	
883 (5)	879 (4)	876 (4)	
976 (3) sh	973 (2) sh	974 (2) sh	

clusters			
$[W_6S_8((2T)_3P)_6]$ ^c	$[W_6S_8(T-PPh_2)_6]$	$[W_6S_8(2T-PPh_2)_6]$	$[W_6S_8(3T-PPh_2)_6]$
329 (23)	233 (165)	231 (163)	231 (119)
859 (0.27) sh	311 (43)	326 (154)	260 (65) sh
	359 (29)	419 (22) sh	375 (128)
	420 (14)	864 (4) sh	864 (3) sh
	864 (4) sh		

^a In dichloromethane, unless otherwise noted, and with units λ_{max}/nm ($\epsilon_{max}/10^3 \cdot L \cdot mol^{-1} \cdot cm^{-1}$). ^b Due to its insolubility, a saturated dichloromethane solution was used and the concentration was not determined ^c In benzonitrile.

addition to these bands attributed to the $[W_6S_8P_6]$ core, all the functionalized clusters present the characteristic $\pi \rightarrow \pi^*$ transition of the thiophene moieties. However, due to the high intensity of the latter, the bands of some of the compounds are sometimes invisible, which complicates the comparison. For example, due to the low solubility and concomitant low concentration of $[W_6S_8(3T-PEt_2)_6]$, only

(56) Scott, T. L.; Wolf, M. O. *J. Phys. Chem. B* **2004**, *108*, 18815–18819.

(57) Becker, R. S.; Seixas de Melo, J.; Maçanita, A. L.; Elisei, F. *J. Phys. Chem.* **1996**, *100*, 18683–18695.

Table 5. CVData (E (V) vs Ag/AgCl) in CH_2Cl_2 for the Ligands^a

ligands							
PPh ₃	T-PEt ₂	2T-PPh ₂	2T-PEt ₂	2EDOT-PPh ₂	2EDOT-PEt ₂	3T-PEt ₂	(2T) ₃ P
1.43	1.43	1.42 1.84	1.16	1.03 1.54	0.95	0.99	1.12

^a The value reported for 3T-PPh₂ is +0.92 V vs SCE.²¹

the band corresponding to the terthiophene moiety can be well observed.

No significant shift for the $\pi \rightarrow \pi^*$ transition can be observed between the clusters and the corresponding uncoordinated ligand except for $[\text{W}_6\text{S}_8((2\text{T})_3\text{P})_6]$ where the ligand $(2\text{T})_3\text{P}$ is blue-shifted 14 nm when coordinated (spectra in Supporting Information). A very small shift (2 nm) was also reported between 3T-PPh₂ and its corresponding complex $\text{PdCl}_2(3\text{T}-\text{PPh}_2)_2$.²¹ Therefore, as observed for the ligands, along the series $[\text{W}_6\text{S}_8(n\text{T}-\text{PR}_2)_6]$ ($n = 1, 2, 3$; R = Et, Ph) the thiophene band is red-shifted with increasing oligomer length and this shift decreases in the same way. The values for both series $[\text{W}_6\text{S}_8(n\text{T}-\text{PEt}_2)_6]$ and $[\text{W}_6\text{S}_8(n\text{T}-\text{PPh}_2)_6]$ are quite similar.

Electrochemical Study. The electropolymerization technique was preferred to the chemical polymerization technique because the latter usually leads to materials of lower quality due to contamination by the catalyst. The proposed mechanism of the electropolymerization of oligothiophene derivatives is the generation of the thiophene cation radical which then reacts with another thiophene molecule. The oxidation potential of the oligomer formed is lower, and as a consequence, the reaction follows on.⁸ Thus, the first oxidation peak potential observed, corresponding to the formation of the radical cation, is irreversible. All the potential values given below are referenced to the Ag/AgCl electrode.

Ligands. The redox properties of the ligands were studied by CV. Electrochemical data obtained are summarized in Table 5. All values correspond to oxidative phenomena and are irreversible processes.

Density functional theory (DFT) calculations have been performed for the phosphinothiophene series $n\text{T}-\text{PPh}_2$ ($n = 1, 2, 3$), and their frontier orbitals were reported.⁵⁶ This study shows that the P lone pair and the thiophene moiety are both involved in the HOMO of the ligand. The phosphorus contribution diminishes as the oligomer length increases, but it is still significant for 3T-PPh₂. The oxidation peaks observed in the CVs are thus both phosphorus- and thiophene-based.

By comparing the ethyl derivatives to the phenyl ones, we find that the first oxidation occurs at a lower potential when bearing ethyl groups. As expected, along the $n\text{T}-\text{PEt}_2$ ($n = 1, 2, 3$) series, the oxidation potential decreases by increasing the oligomer length. 2-EDOT-PEt₂ has a value comparable to that of 3T-PEt₂. As already known, 2EDOT derivatives have a lower oxidation potential compared with that of the 2T species.

For all the ligands studied, upon cycling repeatedly past the first oxidation wave, the peak slowly disappeared, resulting in passivation of the electrode. This phenomenon

has already been observed for other phosphino-thiophene species^{21,48} and has been explained by the reaction of the phosphine group with the oxidized thiophene moiety of another molecule. As already mentioned in the Introduction, the polymerization of thiophene oligomers has been reported to occur primarily by C-C coupling at the α positions. If we consider the α - α coupling to be the main way of connection, the polymerization of T-PR₂, 2T-PR₂, and 3T-PR₂ (R = Et, Ph) must lead to bithiophene (2T), quaterthiophene (4T), and sexithiophene (6T) species, respectively, and not to an extended polymer. This is also true for the EDOT derivatives. In all cases, no electrochemical evidence of these species with lower oxidation potentials has been observed, which suggests, again, that some reaction with the phosphorus atom occurs, preventing any thiophene coupling. For the clusters, the lone pair of the phosphorus atom is involved in the coordination of the metal atom, so in this case this specific reaction should not occur.

Clusters. Given the lower oxidation potentials of 3T-PR₂ (R = Et, Ph) and 2EDOT-PEt₂ ligands, the redox properties of the clusters $[\text{W}_6\text{S}_8(3\text{T}-\text{PR}_2)_6]$ (R = Et, Ph) (**3a,b**) and $[\text{W}_6\text{S}_8(2\text{EDOT}-\text{PEt}_2)_6]$ (**5**) would have been very interesting to study. Unfortunately, no solvent was found to solubilize these clusters and enable such a study. Thus, only the soluble clusters (**1a-2b** and **4**) have been investigated. Note that the polymerization of these species is expected to lead to quaterthiophene groups, as longer conjugated chains, and not to an extended polythiophene polymer.

Clusters based on the $[\text{M}_6\text{Q}_8]$ (M = W, Mo; Q = S, Se) core possess 20 metal-based valence electrons in the neutral state. Their CVs are characterized by two one-electron reversible redox waves, one in reduction and one in oxidation involving the redox couples $[\text{W}_6\text{S}_8]^{+/-0}$ and $[\text{W}_6\text{S}_8]^{0/+}$, respectively. By going to increasingly positive potentials, these clusters undergo two irreversible redox processes. Although the origin of these processes is unknown at present, they are metal and terminal ligand independent. For example, the $[\text{Mo}_6\text{S}_8(\text{tbp})_6]$ cluster also exhibits these two peaks. In general, these processes appear to involve a multi-electron process, and the oxidation of M-S bonds of the $[\text{M}_6\text{S}_8]$ core has been suggested as potentially responsible.⁴⁰

Electrochemical data obtained are summarized in Table 6. The CV of **1b** is shown in Figure 6 and presents five redox waves. By going from cathodic to anodic potentials, it is noted that the first two waves are reversible and the following three are irreversible. For comparison, the CV of $[\text{W}_6\text{S}_8(\text{PEt}_3)_6]$, bearing no thiophene moiety, has been carried out in the same conditions and is reported in the Supporting Information. The latter also displays the classical two reversible waves followed by the two irreversible ones. The

Table 6. CV Data (E (V) vs Ag/AgCl) of the Functionalized Clusters in CH_2Cl_2 . For the Reversible Processes, the Given Values Correspond to $E_{1/2}$

clusters					
$[\text{W}_6\text{S}_8(\text{PEt}_3)_6]$	$[\text{W}_6\text{S}_8(\text{T}-\text{PEt}_2)_6]$ (1b)	$[\text{W}_6\text{S}_8(\text{T}-\text{PPh}_2)_6]$ (1a)	$[\text{W}_6\text{S}_8(2\text{T}-\text{PEt}_2)_6]$ (2b)	$[\text{W}_6\text{S}_8(2\text{T}-\text{PPh}_2)_6]$ (2a)	$[\text{W}_6\text{S}_8((2\text{T})_3\text{P})_6]$ in benzonitrile (4)
-1.28 rev	-1.10 rev	-1.00 rev	-1.06 rev	-1.10 rev	-0.65 rev
0.10 rev	0.19 rev	0.34 rev	0.28 rev	0.38 rev	0.07 irrev
0.92 irrev	0.82 irrev	1.10 irrev	0.75 irrev	1.04 irrev	0.66 irrev
1.41 irrev	1.19 irrev	1.49 irrev	1.05 irrev	1.51 irrev	1.01 irrev
	1.27 irrev	1.65 irrev	1.30 irrev		1.20 irrev

corresponding values (Table 6) are similar to those reported in the literature in THF for this cluster with PEt_3 ligands.²

By comparing the values reported in Table 6 for $[\text{W}_6\text{S}_8(\text{PEt}_3)_6]$ and $[\text{W}_6\text{S}_8(\text{T}-\text{PEt}_2)_6]$, we deduced that the first two reversible peaks of the latter are shifted in the positive direction while the two following irreversible ones are negatively shifted. The additional peak of $[\text{W}_6\text{S}_8(\text{T}-\text{PEt}_2)_6]$ at +1.27 V can be thus attributed to the oxidation of the thiophene-based ligand. After multiple scans, the CV of this cluster remained unchanged. No polymerization occurs for T- PR_2 ligands bearing only one thiophene group, likely due to the steric inaccessibility of the radical formed. No new species are created during the cycling, which shows the stability of this cluster at a potential up to +1.6 V vs Ag/AgCl.

The CV of **1a** is reported in the Supporting Information. It displays the five redox waves observed for $[\text{W}_6\text{S}_8(\text{T}-\text{PEt}_2)_6]$. The peak intensities are lower due to the poor solubility of the cluster in CH_2Cl_2 . All the peak potential values are positively shifted compared with those of the ethyl analogue. This shift is probably due to the attractive effect of the phenyl group compared with that of the ethyl one, a phenomenon already observed for the uncoordinated ligands. As **1b**, the $[\text{W}_6\text{S}_8(\text{T}-\text{PPh}_2)_6]$ cluster did not polymerize.

During the first scan, the CV of **2b** displays several discernible peaks whose values are reported in Table 6 (CV in Supporting Information). The peaks at -1.06 and 0.28 V are actually reversible when the potential is scanned around these values and are attributed to the cluster core. By the

application of multiple scans past +1.30 V, the peaks all progressively disappeared and a film formed on the electrode with a gray metallic aspect. No formation of quaterthiophene units has been observed in the CV, suggesting that no polymerization occurred. The electrochemical behavior of the cluster (the two reversible waves) was not evident for the film on the electrode, indicating that the cluster is not preserved in the film.

The CV of **2a** is quite similar to that of **2b**, but the peak intensities are lower due to its lower solubility (the first scan is reported in the Supporting Information). The first two cluster-centered peaks at -1.10 and +0.38 V are also reversible when the potential is scanned around this value. The peak values are positively shifted compared with that of $[\text{W}_6\text{S}_8(2\text{T}-\text{PEt}_2)_6]$ as observed for the $[\text{W}_6\text{S}_8(\text{T}-\text{PR}_2)_6]$ (R = Et, Ph) clusters. By the application of multiple scans, this cluster behaved like **2b**.

The CV of **4** in benzonitrile presents five oxidation processes in the first scan (Supporting Information). The first wave at -0.65 V is reversible, but the second one at +0.07 V, usually reversible for these clusters, is, in this case, irreversible. The peak values, and especially the one corresponding to the reduction process, are shifted in the positive direction (~ 40 mV) compared with all the clusters studied. The following irreversible redox processes were not well resolved. After multiple scans from 0 to +1.6 V, the peaks disappeared with a concomitant decrease in current. No electrochemical signature of quaterthiophene units or of the cluster core was observed after the first scan.

To sum up, none of the clusters studied underwent electropolymerization. The CVs of these compounds are quite complicated. In all cases, to obtain ligand oxidation, the initially neutral cluster is oxidized twice (the second one is irreversible) to less than 19 electrons, and we do not know how the irreversible oxidations affect the electronic properties of the cluster and its reactivity. For the clusters **2a,b** and **4** bearing ligands with bithiophene groups, it seems that as soon as the ligand gets oxidized the cluster becomes unstable. We can suggest that the ligand-based radical cation formed reacts with the $[\text{W}_6\text{S}_8]^{2+}$ units leading to the cluster core degradation. This reactivity is not observed for clusters coordinated by the T- PR_2 (R = Ph, Et) ligands, since the CVs are reversible. This can be explained by the steric inaccessibility of the radical cation (located on the phosphorus atom and on the thiophene moiety of HOMO), due to the alkyl groups.

In contrast, the electropolymerization of a palladium complex containing 3T-PPh₂ and formulated $\text{PdCl}_2(3\text{T}-$

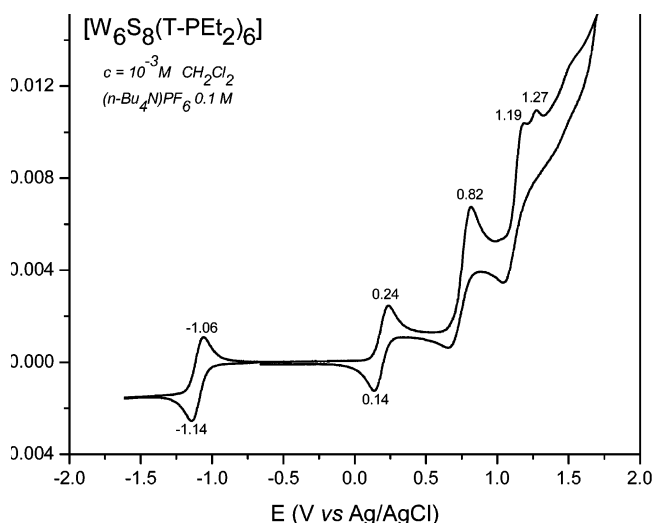


Figure 6. CV of $[\text{W}_6\text{S}_8(\text{T}-\text{PEt}_2)_6]$ in dichloromethane containing 0.1 M $(n\text{-Bu}_4\text{N})\text{PF}_6$ at a scan rate of 200 mV/s.

PPh_2)₂ has been successfully reported.²¹ The comparison is difficult because in this case the nature of the metal center, the charge of the metal center, and the thiophene chain length are different. Again, it would be interesting to investigate the electrochemical behavior of clusters functionalized with the terthiophene moiety.

Electrocrystallization is a technique used to grow crystals of radical cation salts by slow oxidation in solution of the electroactive precursors.⁵⁸ To get a crystalline form of a cluster polymer, several experiments in galvanostatic mode have been performed with $[\text{W}_6\text{S}_8(2\text{T}-\text{PEt}_2)_6]$. Unfortunately, all attempts led, after several weeks, to unidentified amorphous products deposited on the electrode.

Conclusions

We have reported here our new strategy toward the synthesis of an extended network composed of $[\text{W}_6\text{S}_8]$ clusters as building blocks and π -conjugated ligands as electronically active linkers. For this purpose, the octahedral $[\text{W}_6\text{S}_8]$ core has been successfully functionalized with different types of phosphino–thiophene ligands. New phosphino–thiophene ligands and eight original clusters coordinated with these thiophene moieties have been synthesized. Six of them have been characterized by single-crystal X-ray crystallography with up to 36 thiophene units, thus confirming the functionalization of the six apical positions of the $[\text{W}_6\text{S}_8]$ core. These clusters represent an unprecedented series of functionalized clusters. The redox behaviors of both the ligands and the polymerizable clusters were analyzed by CV.

The solubility of the clusters was an issue for their characterizations and especially for the electropolymerization experiments. The replacement of the phenyl groups by ethyl groups on the ligands improved the solubility of the cluster product. Moreover, this substitution appeared to have other several positive effects, such as better reactivity in the coordination reaction and a lower oxidation potential of the thiophene-based ligands. Unfortunately, this substitution was not enough to make the 2-EDOT and 3T-based clusters soluble, clusters which were expected to have the lower

polymerization potentials. The problem is that the solubility and the oxidation potential decrease concomitantly as the thiophene chain length increases.

Electropolymerization experiments of the bithiophene-functionalized clusters were not successful. The exact nature of the reaction occurring between the oxidized bithiophene ligands and the clusters is difficult to evaluate. We know, so far, that no thiophene coupling occurs and the cluster is not preserved. Indeed, at the potential needed to polymerize the ligand, the cluster is overoxidized. The ideal ligand would exhibit a polymerization potential before the irreversible oxidation wave of the cluster core. In this context, molybdenum-based octahedral clusters would be interesting to study because $[\text{Mo}_6\text{S}_8(\text{PEt}_3)_6]$ clusters showed higher oxidation potentials compared with those of the tungsten analogue. However, this would only be effective if the oxidation potential of the ligand is not influenced by the $[\text{Mo}_6\text{S}_8]$ core. Another possibility is to use ligands of different nature. Replacement of the phosphine group by others coordinating site would be interesting to study, not only to modify the oxidation potential of the ligand but also to know if the phosphorus atom is really involved in the cluster instability. Instead of thiophene derivatives, other polymerizable molecules can also be considered.

To conclude, this study demonstrates that the polymerization method is a way to pursue to prepare an extended network of $[\text{W}_6\text{S}_8]$ clusters. As the oxidation of the cluster is required for the network conductivity, the electropolymerization is a good method because the oxidation can be achieved in situ. As already mentioned, many possibilities still remain to be explored to synthesize polymerizable clusters with adequate redox properties, in order to obtain cluster-based extended networks.

Acknowledgment. This work was supported by a grant from the U.S. Department of Energy (DE-FG02-87ER45298). We thank Drs. Min Yuan and Catherine Oertel for helpful discussions about tungsten cluster chemistry.

Supporting Information Available: X-ray crystallographic files (CIF) and other characterization data (PDF). This material is available free of charge via the Internet at <http://pubs.acs.org>.

IC7010748

(58) Montgomery, L. K. *Organic Conductors, Fundamentals and Applications*; Farges, J.-P., Ed.; Marcel Dekker: New York, 1994; p 115.